








RESEARCH ARTICLE | APRIL 03 2024

Feasibility of GaAs/AlGaAs quantum cascade laser operating above 6 THz

D. V. Ushakov ; A. A. Afonenko ; An. A. Afonenko ; R. A. Khabibullin; M. A. Fadeev ; V. I. Gavrilenko ; A. A. Dubinov  

 Check for updates

J. Appl. Phys. 135, 133108 (2024)

<https://doi.org/10.1063/5.0198236>

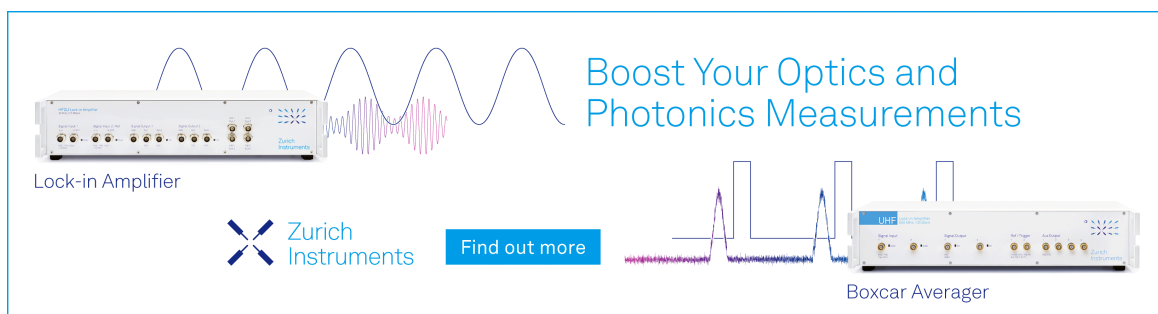


View Online




Export Citation

03 April 2024 12:54:10



Boost Your Optics and Photonics Measurements

Lock-in Amplifier

 Zurich Instruments

[Find out more](#)

Boxcar Averager

Feasibility of GaAs/AlGaAs quantum cascade laser operating above 6 THz

Cite as: J. Appl. Phys. 135, 133108 (2024); doi: 10.1063/5.0198236

Submitted: 17 January 2024 · Accepted: 19 March 2024 ·

Published Online: 3 April 2024



D. V. Ushakov,¹ A. A. Afonenko,¹ An. A. Afonenko,¹ R. A. Khabibullin,² M. A. Fadeev,³ V. I. Cavrilenko,^{3,4} and A. A. Dubinov^{3,5,a)}

AFFILIATIONS

¹Faculty of Radiophysics and Computer Technologies, Belarusian State University, Minsk, Belarus

²Mokerov Institute of Ultrahigh Frequency Semiconductor Electronics, Moscow, Russia

³Institute for Physics of Microstructures RAS, Nizhny Novgorod, Russia

⁴Advanced School of General and Applied Physics, Lobachevsky State University of Nizhny Novgorod, Nizhny Novgorod, Russia

⁵Faculty of Radiophysics, Lobachevsky State University of Nizhny Novgorod, Nizhny Novgorod, Russia

^{a)}Author to whom correspondence should be addressed: sanya@ipmras.ru

ABSTRACT

A band design of a quantum cascade laser with a generation frequency higher than 6 THz and an active region based on four GaAs/Al_{0.14}Ga_{0.86}As quantum wells is proposed. Calculations were carried out based on the solution of the Schrödinger equation taking into account the dephasing of quantum states, as well as a closed system of balance equations. The temperature dependences of the gain at frequencies of 6.3–6.6 THz were calculated for the proposed quantum cascade laser with a double metal waveguide. Features of the proposed laser structure include two injection quantum wells and the suppression of non-radiative transitions between laser levels. According to calculations, this provides the maximum operating temperature of up to 81 K at 6.4 THz. The results of this study open up the way for quantum cascade lasers based on GaAs/AlGaAs to operate at frequencies above 6 THz.

© 2024 Author(s). All article content, except where otherwise noted, is licensed under a Creative Commons Attribution (CC BY) license (<https://creativecommons.org/licenses/by/4.0/>). <https://doi.org/10.1063/5.0198236>

INTRODUCTION

For 21 years of their existence, terahertz quantum cascade lasers (THz QCLs) have achieved significant progress, in terms of both maximum operating temperatures and their output power.^{1–3} However, there is a frequency range (6–10.5 THz) where QCLs are still unable to operate. On the low-frequency side of this inaccessible range, the maximum cutoff frequency of 6 THz was achieved in GaAs/Al_{0.25}Ga_{0.75}As QCL;⁴ on the high-frequency side, a cutoff frequency of 10.5 THz was achieved in In_{0.53}Ga_{0.47}As/GaAs_{0.51}Sb_{0.49} QCL.⁵ There are two main factors that contribute to the absence of QCLs with a frequency between 6 and 10.5 THz.⁶ The first one is the optical phonon absorption in semiconductors which QCLs are made of (GaAs/AlGaAs, InGaAs/InAlAs/GaAsSb). The second factor is the increased rate of nonradiative relaxation of electrons from the upper to the lower laser level by the emission of a LO-phonon. Note that the development of QCLs operating in the frequency range under consideration is important for various practical applications (see, for example, review).⁷

Therefore, semiconductor heterostructures with different optical phonon frequencies were proposed as an active medium of QCLs alternative to arsenides, which include GaInP/AlGaInP,⁸ GaN/AlGaIn,⁹ ZnO/MgZnO,¹⁰ ZnSe/ZnMgSe,¹¹ and HgCdTe.¹² However, owing to the relative novelty of these material systems, the lasing is yet to be observed at temperatures above ~5 K.¹³ For other heterostructures, only spontaneous emission has been observed.^{14,15}

In this work, we show that the capabilities of GaAs/AlGaAs heterostructures with quantum wells (QWs) are wider than previously thought.⁶ We investigate the possibility of making such a design of the GaAs/AlGaAs-based QCL with a double metal waveguide, which provides lasing with a frequency of more than 6 THz at temperatures above the temperature of liquid nitrogen (77 K).

MODEL AND RESULTS OF CALCULATION

There are several methods for calculating QCL characteristics, for example, the non-equilibrium Green function (NEGF) method¹⁶ and the Monte-Carlo/Density matrix (MCDM)

03 April 2024 12:54:10

method.^{17,18} To model the THz QCL based on GaAs/AlGaAs, we found a numerical solution to a system of balance equations for localized states and continuum states. In order to account for the effects of dephasing on the processes of the charge transport, we employed the technique of modifying the eigenbasis of the Schrödinger equation by reducing the dipole moments of tunnel-bound states. The algorithm for calculating optoelectronic properties includes (a) determining the energy levels and wave functions based on the solution of the Schrödinger equation within three-band $\mathbf{k}\cdot\mathbf{p}$ -approximation, calculating the matrix elements of dipole transitions; (b) calculating tunneling rates and scattering rates on optical phonons, ionized impurities, roughness of heteroboundaries and an electron–electron scattering; (c) determining surface concentrations of carriers for the corresponding energy subbands from the closed system of balance equations; and (d) calculating the electric current, gain and absorption spectra, and output radiation power. The details of the calculation method tested on several GaAs/AlGaAs QCL designs and a comparison of the calculations with experimental results showing good agreement can be found in Refs. 19 and 20. Also, we made the test calculations for the recent experimental structures of 5.3–5.6 THz spectral range⁴ and found good agreement in the prediction of the generation frequency and the threshold current.

To search for high-frequency (over 6 THz) laser heterostructures, we optimized the designs with four and five QWs in a cascade by scanning the thicknesses of QWs and $\text{Al}_x\text{Ga}_{1-x}\text{As}$ barrier layers with different compositions x . Figure 1 shows the conduction band diagrams, the energy levels, and the squared modules of wave functions of an optimized design with four QWs in a cascade with a sequence of layers: 5.64/14.39/4.80/7.90/4.52/6.49/4.23/8.75 nm ($\text{Al}_{0.14}\text{Ga}_{0.86}\text{As}$ barriers are indicated in italics). The widest QW is n-doped with a layer concentration of $4.6 \times 10^{10} \text{ cm}^{-2}$.

The optimal mole composition of aluminum in the barrier layers found during the scanning for the maximum operating temperature is ($x = 0.14$). It enables the widest possible barriers to minimize the scattering at the roughness of heterointerfaces and limits the leakage of electrons into the continuum states resulting in higher output power and operating temperature. The design with five QWs in a cascade with two extractors showed a similar maximum operating temperature compared to the design with four QWs and a single extractor and did not demonstrate any clear advantages.

In one cascade, carrier transfer and operating laser transitions involve the states of the following levels: injectors (i) and (i_2), upper (u) laser level, and lower (le) laser level, which also serves as an extractor. The upper laser level (u) is tunnel-coupled to the injector level (i_2) for the efficient transfer of the electrons between cascades. The injector level (i_2) is in turn strongly coupled to the injector (i). An additional injection QW is required to accumulate the energy of a high-frequency laser transition ($u-le$) (>6 THz) at an applied voltage. In this case, populations N_{2D} of levels (i), (i_2), and (u) are 37%, 8%, and 41% of the total electron concentration, respectively. The lower laser level (le) is weakly populated ($\sim 13\%$), and as long as it plays the role of an extractor, it is located higher in energy than the injector level (i') by approximately the energy of the phonon for effective diagonal depletion.

As stated above, the problem of creating high-frequency QCLs is the absorption near the phonon resonance and it is crucial to minimize its influence on the gain in the region of high-frequency generation. In a conventional resonance-phonon design with a lasing frequency of up to 5 THz, the second level [level (p) in Fig. 1] of the wide QW is tunnel-coupled to the lower laser level and acts as an extractor,^{21,22} without affecting the gain in the lasing region. At frequencies above 6 THz, this level is parasitic, because absorption due to the resonance-phonon transition greatly weakens the generation channel ($u-le$). As can be seen from Fig. 1(b), an important feature of the proposed design is that the energy gap

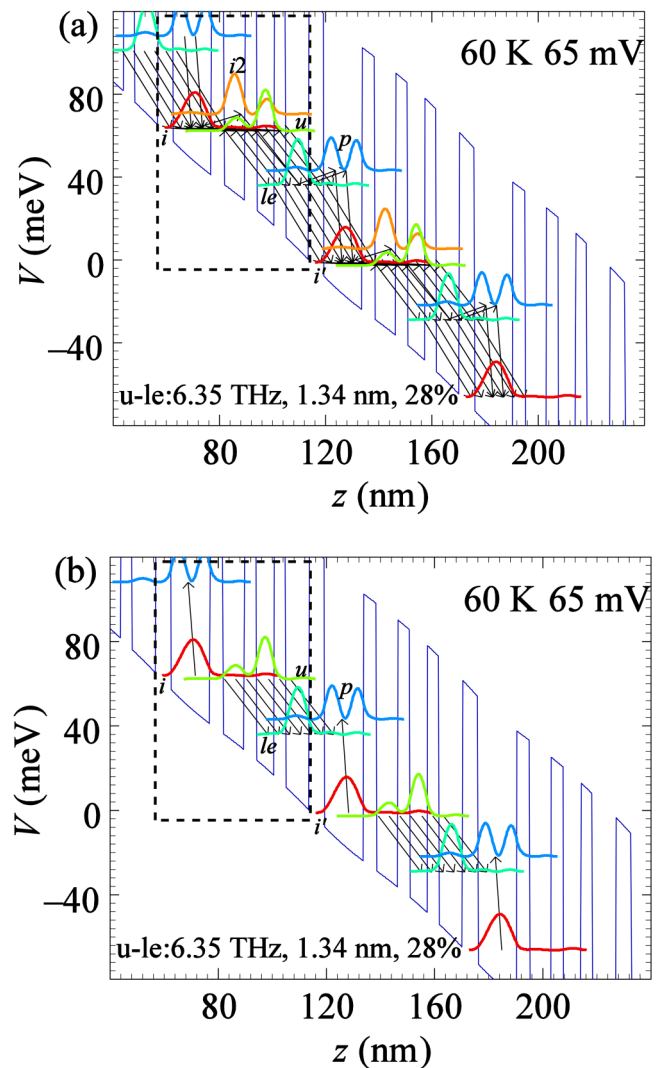


FIG. 1. Conduction band diagrams and squared moduli of electron wave functions for an optimized THz QCL based on GaAs/ $\text{Al}_{0.14}\text{Ga}_{0.86}\text{As}$ at a temperature of $T = 60 \text{ K}$, $V_1 = 65 \text{ mV}$, $\nu_{u-le} = 6.35 \text{ THz}$ and $Z_{u-le} = 1.34 \text{ nm}$. The arrows show the direction of current flow (a) and radiative transitions (b).

03 April 2024 12:54:10

TABLE I. Energies, level populations, and scattering parameters for various mechanisms at $V_1 = 65$ mV calculated using methods from Refs. 19 and 20.

Levels	E (meV)	N_{2D}	γ_{tun} (meV)	γ_{phon} (meV)	γ_{imp} (meV)	γ_{rough} (meV)	γ (meV)
i	0	0.38	0.10	0.00	0.06	0.03	0.39
i_2	6.5	0.083	0.00	0.03	0.07	0.20	0.50
u	-1.6	0.41	0.07	0.01	0.03	0.07	0.39
le	-27.8	0.13	0.00	0.08	0.02	0.01	0.31
p	-20.7	0.004	0.00	0.97	0.09	0.09	1.34

between the injector (i) and the parasitic level (p) of the wide QW is increased to 44 meV, which is larger than the optical phonon energy of 37 meV, significantly reducing the radiation absorption in channel (i - p) while also minimizing the broadening of the lower laser level due to weak coupling with it ($\Delta E_{p-le} \approx 7$ meV).

The gain spectrum was determined similarly to Refs. 19 and 20, taking into account the contribution of non-resonant transitions,

$$G(\nu) = \frac{2\pi^2 e^2 \nu}{\epsilon_0 c n_r d} \sum_{E_i > E_j} |z_{ij}|^2 (n_i - n_j) [F_{ij}(h\nu, E_i - E_j) - F_{ij}(h\nu, E_j - E_i)], \quad (1)$$

where ν is the radiation frequency, c is the speed of light in vacuum, h is Planck's constant, n_r is the refractive index of the active region, ϵ_0 is the dielectric constant of vacuum, d is the period of the structure, and $n_{i,j}$ and $E_{i,j}$ are the two-dimensional concentrations of charge carriers and the energies of levels i and j . The form factor of the spectral line was taken in the form of a modified Lorentz contour,

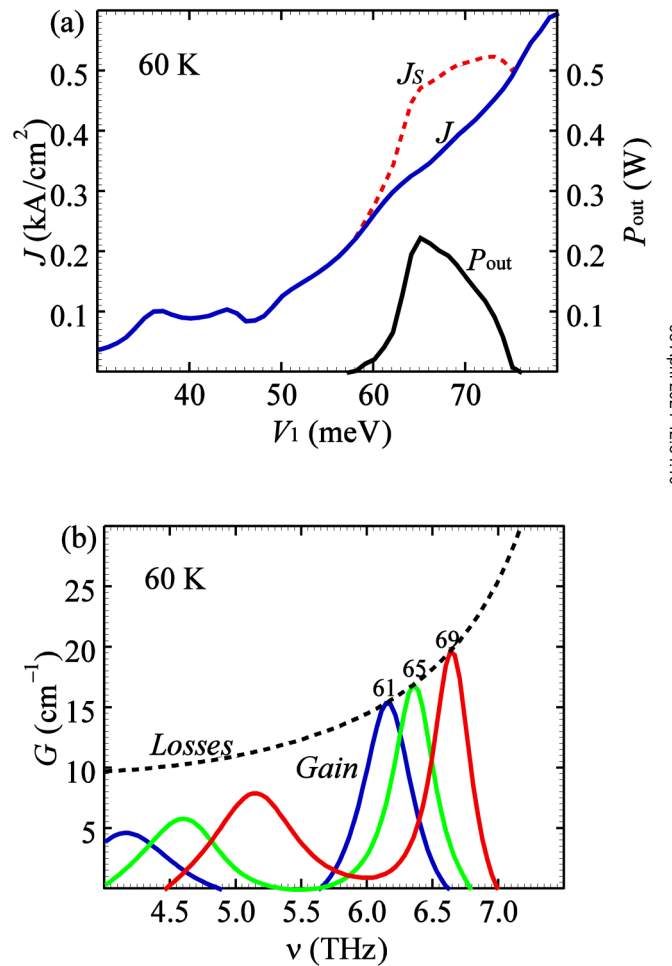
$$F_{ij}(h\nu, \Delta E) = \frac{\gamma_{ij}}{\pi} \cdot \frac{1}{(h\nu - \Delta E)^2 + \gamma_{ij}^2} \cdot \frac{2}{\left(1 + \exp\left(\frac{h\nu - \Delta E}{k_B T}\right)\right) \left(1 + \exp\left(-\frac{h\nu + \Delta E}{k_B T}\right)\right)}, \quad (2)$$

where k_B is Boltzmann's constant and T is the temperature. Here, $\gamma_{ij} = \gamma_i + \gamma_j$ is the total broadening parameter, which accounts for the lifetimes of levels i and j . The broadening parameter for the selected level i includes the components of scattering by tunneling (γ_{tun}), scattering by optical phonons (γ_{phon}), impurities (γ_{imp}), heterointerface roughness (γ_{rough}), electron-electron scattering (γ_{ee}), and spatial inhomogeneity broadening (γ_{sp}),

$$\gamma = \gamma_{\text{tun}} + \gamma_{\text{phon}} + \gamma_{\text{imp}} + \gamma_{\text{rough}} + \gamma_{ee} + \gamma_{\text{sp}}. \quad (3)$$

The optical phonon scattering was calculated using GaAs-, AlAs-, and AlGaAs-like bulk modes.²³⁻²⁵ The estimated value of electron-electron scattering and spatial inhomogeneity broadening was assumed to be 0.1 meV for all operating levels. For the roughness scattering, we used 0.3 and 9 nm for the root mean square thickness and correlation length that were estimated from our analysis of experimental data from Ref. 4.

High gain in the proposed design is achieved by minimizing the spectral broadening of the radiative laser transition (u - le) due to the influence of non-radiative transitions arising from tunneling, scattering by phonons, by impurities, and by heterointerface


FIG. 2. (a) Current-voltage and output power characteristics for the structure with lasing (J_s) and without lasing (J) and (b) spectra of the gain and losses in the lasing regime for various voltages on one active cascade V_1 (numbers on the curves) in the range of the positive branch of the current-voltage characteristic.

roughness. Table I presents the main dissipation parameters for operating levels in one cascade in the proposed optimal design. As can be seen, for laser levels (u) and (le), the total scattering value is 0.31–0.39 meV, which is achieved thanks to thick adjacent barriers of the QW containing the lower laser level (le) and selective doping of the wide QW.

It should be noted that dephasing effects play a dominant role in the transfer between weakly bound states.^{19,26–28} An increase in the injector barrier thickness leads to the loss of coherence of eigenenergy states and reduces the efficiency of electron transport through the injector.²⁷ In Ref. 27, the dependence of the current density on the thickness of the tunnel barrier for GaAs/Al_{0.3}Ga_{0.7}As superlattice was studied within the framework of the density matrix formalism. It was shown that the approximation of strong coupling works for the difference in intrinsic energies of less than 3 meV. In this work, the basis states are localized in individual QWs, which ensures their coherence.¹⁹ For this case, the probability of the tunneling i - u through is $5.0 \times 10^{11} \text{ s}^{-1}$ at an operating voltage of 65 mV. A wide barrier of 4.5 nm between the laser levels (u) and (le) ensures a low probability of a non-radiative (u - le) transition ($\sim 7.7 \times 10^{10} \text{ s}^{-1}$), which is necessary to maintain the population inversion under the condition of a relatively high probability of depletion of the lower laser level ($\sim 2.5 \times 10^{11} \text{ s}^{-1}$). This also leads to a smaller diagonal matrix element of the laser transition $Z_{u-le} = 1.34 \text{ nm}$ compared to lower frequency lasers ($Z_{u-l} \sim 3\text{--}4 \text{ nm}$), which, however, is sufficient to overcome the total losses of $\sim 15\text{--}25 \text{ cm}^{-1}$. A description of the calculation of losses is given below.

The calculations assumed that GaAs/AlGaAs QCL with 3 mm length and $100 \mu\text{m}$ width and the active region with a thickness of $10 \mu\text{m}$ (176 cascades and optical limiting factor is close to 1) is contained in a symmetrical waveguide with 50 nm thick n^+ -GaAs contact layers doped with a concentration of $5 \times 10^{18} \text{ cm}^{-3}$ and Au/Ti(10 nm)-Ti(10 nm)/Au metal plates.

Figure 2 shows the calculated current–voltage characteristics and the gain spectra in the lasing regime for various voltages on one active cascade V_1 . The current–voltage characteristic has additional “parasitic” peaks at the voltage below the lasing threshold of 37 and 45 mV, which are associated with resonant tunneling of electrons between the injectors (i_1 , i_2) and extractor (le) levels. The gain in the design under consideration occurs on the positive differential resistance branch of the current–voltage characteristic, which is necessary to fulfill the condition of electrical stability at the operating point. The large positive differential resistance range of V–I characteristic is achieved by the large energy detuning from the tunneling resonance between the injector levels i_1 and i_2 . It is important to note the width of the range of the positive branch of the photon assisted current curve J_s in the lasing regime at voltages of $\sim 59\text{--}73 \text{ mV}$, which is associated with stimulated transitions of electrons and covers the wide spectral range of $\sim 6.1\text{--}6.6 \text{ THz}$. The wide range of generation frequency tuning ($\sim 0.5 \text{ THz}$) depending on the applied voltage is due to a high generation frequency and slower change in the energy of the upper laser level (u) compared to the lower one (le).

In order to estimate the maximum operating temperatures of the given design, we calculate the complex dielectric function and cavity losses as a function of temperature using the method proposed in Refs. 29 and 30. This calculation includes losses on the

metal, optical phonons, and free charge carriers. In addition to waveguide mode losses, losses due to the reflection on mirrors were taken into account. For a resonator with 3 mm length and $100 \mu\text{m}$ width, the reflection coefficient is 0.55³¹ and the losses associated with radiation output are 2 cm^{-1} . Figure 3 shows the temperature dependences of the maximum gain and total losses at lasing frequencies of 6.1–6.6 THz, and the output radiation power in the lasing regime for the design under study. The theoretical maximum operating temperature of the laser was determined as the intersection point of the calculated temperature dependences of the total loss coefficient in the cavity and the gain. For voltages of 61, 65, and 69 mV, the calculated values of the maximum operating temperature were 65, 81, and 77 K, respectively, reaching a maximum for the frequency range 6.3–6.6 THz. For a frequency of 6.4 THz,

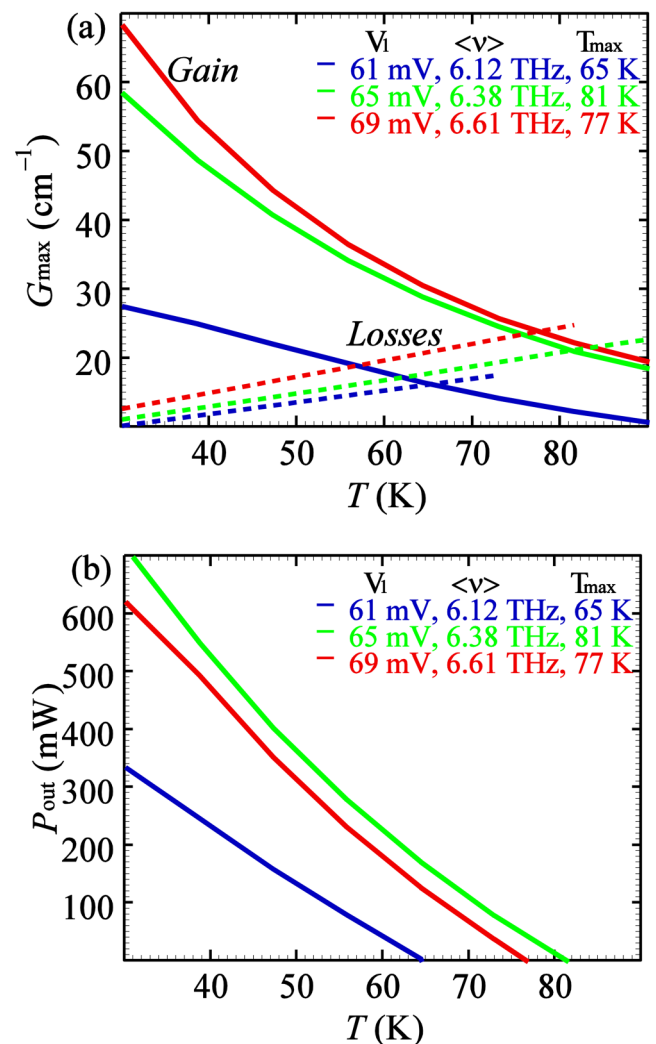


FIG. 3. Temperature dependences of maximum gain (solid curves) and total losses (dashed curves) (a) and output power (b).

03 April 2024 12:54:10

the maximum power values are reached, which at a temperature of 60 K amount to ~ 226 mW. A significant performance drop at 61 meV bias is related to the proximity of the threshold voltage. The full lasing range falls on the positive differential resistance range of V–I characteristic that allows uncontrolled inhomogeneous excitation of the active region near the maximum of L–V characteristic without a risk to fall into the negative differential resistance region.

CONCLUSION

A new QCL design with a generation frequency higher than 6 THz and an active region based on four GaAs/Al_{0.14}Ga_{0.86}As quantum wells is proposed. The main features of the proposed laser structure are two injection quantum wells and suppression of non-radiative transitions for laser levels. The optical gain, losses, and current density change of the QCL are studied theoretically using the three-band k-p-method and balance equations method taking into account the processes of dephasing on the basis of wave functions. Our simulation shows that the suggested QCL is promising for obtaining lasing at frequencies in the region of 6.3–6.6 THz. It is shown that the maximum operating temperature of such a QCL is about 81 K. The new design of QCLs based on GaAs/AlGaAs opens the way for QCLs to advance into the region of operating frequencies above 6 THz.

ACKNOWLEDGMENTS

The work was sponsored by the Russian Science Foundation (Grant No. 23-19-00436). Calculations related to the roughness of hetero-boundaries were performed as part of the project of the BRFB-RSF (Grant No. 24-49-10004).

AUTHOR DECLARATIONS

Conflict of Interest

The authors have no conflicts to disclose.

Author Contributions

D. V. Ushakov: Conceptualization (equal); Data curation (equal); Formal analysis (equal); Investigation (equal); Methodology (equal); Software (equal); Validation (equal); Visualization (equal); Writing – original draft (equal); Writing – review & editing (equal). **A. A. Afonenko:** Conceptualization (equal); Data curation (equal); Formal analysis (equal); Investigation (equal); Methodology (equal); Software (equal); Validation (equal); Visualization (equal); Writing – original draft (equal); Writing – review & editing (equal). **An. A. Afonenko:** Investigation (equal); Software (equal). **M. A. Fadeev:** Investigation (equal); Writing – original draft (equal); Writing – review & editing (equal). **V. I. Gavrilenko:** Formal analysis (equal); Supervision (equal). **A. A. Dubinov:** Conceptualization (equal); Data curation (equal); Formal analysis (equal); Funding acquisition (lead); Investigation (equal); Project administration (lead); Supervision (equal); Validation (equal); Writing – original draft (equal); Writing – review & editing (equal).

DATA AVAILABILITY

The data that support the findings of this study are available from the corresponding author upon reasonable request.

REFERENCES

- ¹A. Khalatpour, M. C. Tam, S. J. Addamane, J. Reno, Z. Wasilewski, and Q. Hu, *Appl. Phys. Lett.* **122**, 161101 (2023).
- ²A. Khalatpour, A. K. Paulsen, C. Deimert, Z. R. Wasilewski, and Q. Hu, *Nat. Photonics* **15**, 16 (2021).
- ³L. H. Li, L. Chen, J. R. Freeman, M. Salih, P. Dean, A. G. Davies, and E. H. Linfield, *Electron. Lett.* **53**, 799 (2017).
- ⁴M. Shahili, S. J. Addamane, A. D. Kim, C. A. Curwen, J. H. Kawamura, and B. S. Williams, *Nanophotonics* (published online 2024).
- ⁵K. Ohtani, M. Beck, M. J. Süess, J. Faist, A. M. Andrews, T. Zederbauer, H. Detz, W. Schrenk, and G. Strasser, *ACS Photonics* **3**(12), 2280 (2016).
- ⁶M. Wienold, B. Roben, X. Lu, G. Rozas, L. Schrottke, K. Biermann, and H. T. Grahn, *Appl. Phys. Lett.* **107**, 202101 (2015).
- ⁷A. Leitenstorfer, A. S. Moskalenko, T. Kampfrath *et al.*, *J. Phys. D: Appl. Phys.* **56**, 223001 (2023).
- ⁸D. V. Ushakov, A. A. Afonenko, R. A. Khabibullin, M. A. Fadeev, and A. A. Dubinov, *Phys. Status Solidi RRL* **18**, 2300392 (2024).
- ⁹L. Wang, T.-T. Lin, M.-X. Chen, K. Wang, and H. Hirayama, *Appl. Phys. Exp.* **14**, 112003 (2021).
- ¹⁰E. Bellotti, K. Driscoll, T. D. Moustakas, and R. Paiella, *J. Appl. Phys.* **105**, 113103 (2009).
- ¹¹V. P. Sirkeli, O. Yilmazoglu, F. Küppers, and H. L. Hartnagel, *Phys. Status Solidi. RRL* **11**, 1600423 (2017).
- ¹²A. A. Dubinov, D. V. Ushakov, A. A. Afonenko, R. A. Khabibullin, M. A. Fadeev, and S. V. Morozov, *Opt. Lett.* **47**, 5048 (2022).
- ¹³W. Terashima and H. Hirayama, *Proc. SPIE* **9483**, 948304 (2015).
- ¹⁴W. Terashima and H. Hirayama, *Phys. Status Solidi C* **8**, 2302 (2011).
- ¹⁵B. Meng, B. Hinkov, N. M. L. Biavan, H. T. Hoang, D. Lefebvre, M. Hugues, D. Stark, M. Franckie, A. Torres-Pardo, J. Tamayo-Arriola, M. M. Bajor, A. Hierro, G. Strasser, J. Faist, and J. M. Chauveau, *ACS Photonics* **8**, 343 (2021).
- ¹⁶H. Yasuda, T. Kubis, P. Vogl, N. Sekine, I. Hosako, and K. Hirakawa, *Appl. Phys. Lett.* **94**, 151109 (2009).
- ¹⁷I. Bhattacharya, C. W. I. Chan, and Q. Hu, *Appl. Phys. Lett.* **100**, 011108 (2012).
- ¹⁸C. Jirauschek, *J. Appl. Phys.* **122**, 133105 (2017).
- ¹⁹D. V. Ushakov, A. A. Afonenko, A. A. Dubinov, V. I. Gavrilenko, O. Y. Volkov, N. V. Shchavruk, D. S. Ponomarev, and R. A. Khabibullin, *Quant. Electron.* **49**, 913 (2019).
- ²⁰D. Ushakov, A. Afonenko, R. Khabibullin, D. Ponomarev, V. Aleshkin, S. Morozov, and A. Dubinov, *Opt. Exp.* **28**, 25371 (2020).
- ²¹H. Luo, S. R. Laframboise, Z. R. Wasilewski, G. C. Aers, H. C. Liu, and J. C. Cao, *Appl. Phys. Lett.* **90**, 041112 (2007).
- ²²B. S. Williams, *Nat. Photonics* **1**, 517 (2007).
- ²³S. G. Yu, K. W. Kim, M. A. Stroschio, G. J. Iafrate, J.-P. Sun, and G. I. Haddad, *J. Appl. Phys.* **82**, 3363 (1997).
- ²⁴M. V. Kisin, M. A. Stroschio, G. Belenky, V. B. Gornkel, and S. Luryi, *J. Appl. Phys.* **83**, 4816 (1998).
- ²⁵A. A. Afonenko, A. A. Afonenko, D. Ushakov, and A. A. Dubinov, *Semiconductors* **54**(8), 936 (2020).
- ²⁶R. A. Kazarinov and R. A. Suris, *Sov. Fiz. Tekh. Poluprovodn.* **5**, 797 (1971).
- ²⁷H. Callebaut and Q. Hu, *J. Appl. Phys.* **98**, 104505 (2005).
- ²⁸S. Kumar and Q. Hu, *Phys. Rev. B* **80**, 245316 (2009).
- ²⁹Y. J. Han, L. H. Li, J. Zhu, A. Valavanis, J. R. Freeman, L. Chen, M. Rosamond, P. Dean, A. G. Davies, and E. H. Linfield, *Opt. Exp.* **26**, 3814 (2018).
- ³⁰D. V. Ushakov, A. A. Afonenko, A. A. Dubinov, V. I. Gavrilenko, I. S. Vasil'evskii, N. V. Shchavruk, D. S. Ponomarev, and R. A. Khabibullin, *Quant. Electron.* **48**, 1005 (2018).
- ³¹S. Kohen, B. S. Williams, and Q. Hu, *J. Appl. Phys.* **97**, 053106 (2005).